

## Study of the Electronic Excited States of Tetrahalomercurate Complex Ions, $[\text{HgX}_4]^{2-}$ . Magnetic Circular Dichroism Spectroscopy and Use of All-Center Angular Momentum Matrix<sup>1</sup>

J. D. GUNTER, A. F. SCHREINER,\* and R. S. EVANS

Received July 23, 1974

AIC40495F

Magnetic circular dichroism (MCD) and electronic absorption spectra show that the lowest energy, intense electronic absorption band (band  $\alpha$ ) of each  $d^{10}$  complex,  $[\text{HgCl}_4]^{2-}$ ,  $[\text{HgBr}_4]^{2-}$ , and  $[\text{HgI}_4]^{2-}$ , derives from the excitation of a ligand-localized  $\pi$ -type MO to a metal-localized, vacant  $a_1^*$  ( $\sim 6s$ ) or  $t_2^*$  ( $\sim 6p$ ). More specifically, of the six  $\pi \rightarrow M$  excitations four are electric dipole allowed,  $^1A_1 \rightarrow ^1T_2$ . The MCD data assert that two of the possible four are ruled out because their Faraday  $A$  terms have the wrong signs. One is then left with the possibility that the lowest energy band is due to either  $^1T_2^B[3t_2^5t_2^*]$  or  $^1T_2^C[e^3t_2^*]$ , since each is predicted to have a large positive  $A/D$  ratio as found from our experiment. The next intense band (band  $\beta$ ) toward higher energy was observed for one of the complexes,  $[\text{HgI}_4]^{2-}$ , and it is at 37.17 kK; it also has a large positive  $A/D$  ratio so that it is perhaps the other of the two possible states mentioned,  $^1T_2^C$  or  $^1T_2^B$ . The magnitudes of excited-state orbital angular momenta are found to be composed almost entirely (98%) of two-center integrals,  $\langle \chi_i(X) | L_z(\text{Hg}) | \chi_j(X) \rangle$ , involving halogen  $s$  and  $p$  valence orbitals.

### Introduction

The interpretation of electronic excitations of the tetrahedral complexes of  $\text{Hg}^{2+}$ , or  $[\text{HgX}_4]^{2-}$ , where  $X^- = \text{Cl}^-$ ,  $\text{Br}^-$ , or  $\text{I}^-$ , has received little attention. This is in part, perhaps, due to the few absorption bands accessible in their appropriate solvent media. These complex ions are of the  $d^{10}$  type; they are tetrahedral, and they have remarkably high stability constants as shown by Marcus.<sup>2</sup> For example, in the presence of excess  $\text{I}^-$  one may quantitatively analyze<sup>3</sup> for  $\text{Hg}^{2+}$  by the formation of  $[\text{HgI}_4]^{2-}$ . Fromherz and Lih<sup>4</sup> obtained the electronic absorption band positions and their molar extinction coefficients in aqueous solution containing excess alkali halide. Tsuchida<sup>5</sup> also attempted to understand  $[\text{HgI}_4]^{2-}$  specifically.

The present report is the first attempt at analyzing the nature of the excited-state structure of  $[\text{HgX}_4]^{2-}$  by magnetic circular dichroism (MCD) spectroscopy<sup>6</sup> along with electronic absorption data. In fact, electronic excited states of tetrahedral complexes of  $d^{10}$  metal ions have previously not been analyzed by means of the potentially powerful MCD spectroscopy. In order to elucidate the excitations,  $a \rightarrow j$ , excited-state orbital angular momentum,  $\langle j | \hat{L}_z | j \rangle$ , which employs the complete many-center operator matrix, and four concisely constructed state functions composed of semiempirical molecular orbitals are used.

### Experimental Section

The MCD spectra were obtained on a JASCO ORD/UV/CD-5 with the SS-20 electronics modification and with a new Baird-Atomic KDP  $1/4 \lambda$  modulator in place of the original ADP unit. Spectra and base lines were scanned several times, and a modification of the JASCO was used for transmission of the analog signal to a Varian C-1024 time-averaging computer, where it was converted to digital form, averaged, and stored. The digital data were punched on paper tape (TMC-TALLY 420 Perforator) and transmitted to a IBM 370/165 via a DATA 100 Tape Reader and a CODEX 4800 DATA CODEM interface unit. The averaged spectra were plotted with a CALCOMP plotter. Five to sixteen scans of MCD spectra were used for the averaging procedure.

Aqueous solutions of  $[\text{HgX}_4]^{2-}$  were obtained by using an appropriate  $\text{Hg}(\text{II})$  compound and a high concentration of alkali halides to give a solution with an absorbance of about unity.  $[\text{HgCl}_4]^{2-}$  was prepared by dissolving  $\text{HgCl}_2$  in 5  $M$   $\text{LiCl}$  solution.<sup>4</sup>  $[\text{HgBr}_4]^{2-}$  was prepared by dissolving  $(\text{NMe}_4)_2[\text{HgBr}_4]$ <sup>7</sup> in 8  $M$   $\text{LiBr}$  solution.  $[\text{HgI}_4]^{2-}$  solution was prepared by dissolving  $(\text{NMe}_4)_2[\text{HgI}_4]$ <sup>7</sup> in 5  $M$   $\text{KI}$  solution.

To eliminate the possibility of the small shoulder on the low-energy intense band (ca. 282 nm) of  $[\text{HgBr}_4]^{2-}$  being caused by a solution impurity species, we also measured the electronic and MCD spectra of solid  $(\text{NMe}_4)_2[\text{HgBr}_4]$  in a Kel-F No. 90 fluorocarbon mull. Also, the MCD spectrum through the higher energy intense band (269 nm)

of  $[\text{HgI}_4]^{2-}$  was not accessible in aqueous  $\text{KI}$  solution due to absorption by the  $\text{I}^-$ -solvent system but it was measurable in a Kel-F mull of solid  $(\text{NMe}_4)_2[\text{HgI}_4]$ .

### Computations

The molecular MCD Faraday ratios,  $A/D$ , were computed as follows in the coparallel coordinate system of Figure 1. The Faraday ratios,  $A/D$ , required the evaluation of one-, two-, and three-center orbital angular momentum integrals,  $\langle \chi_i | \hat{L}_z | \chi_j \rangle$ , chosen here with  $z$  quantization, or  $\langle L_z \rangle$ . This complete matrix,  $L_z$ , over the entire 25 AO's (multi- $\zeta$  metal, single- $\zeta$  ligand)<sup>8</sup> was evaluated as described in detail elsewhere.<sup>9</sup> The operator procedure accounts for all metal-ligand and ligand-ligand, as well as the self-center integral contributions. The Faraday ratios were computed subsequent to transforming the operator matrix,  $L$ , into molecular orbital space using all MO's,<sup>9</sup> followed by computing the quantity  $A/D$  over state functions which form bases of the  $T_d$  point group of the  $C_2$  quantization. For example, for the electric dipole allowed excitations,  $^1A \rightarrow ^1T_2$ , one has

$$A/D = i \langle ^1T_2 \xi | \hat{L}_z | ^1T_2 \eta \rangle$$

where  $^1T_2$  is one of the excited states. We derive the expression by using the  $A$ -parameter expression in the complex basis,<sup>6</sup> converting it to the form of the equivalent real basis, and simplifying by symmetry.<sup>10</sup> For example, if we consider the excited configuration  $t_2^5 a_1^*$ , the excited-state  $^1T_2$  components to be used in the  $A/D$  expression are

$$|^1T_2 \xi \rangle = 1/\sqrt{2} [ | \bar{\xi} \bar{a}_1 \bar{\eta} \bar{\zeta} \bar{\zeta} | + | a_1 \bar{\xi} \bar{\eta} \bar{\zeta} \bar{\zeta} | ]$$

$$|^1T_2 \eta \rangle = 1/\sqrt{2} [ | \bar{\zeta} \bar{\zeta} \bar{\eta} a_1 \bar{\zeta} \bar{\zeta} | + | \bar{\xi} \bar{\xi} a_1 \bar{\eta} \bar{\zeta} \bar{\zeta} | ]$$

where the vertical bars symbolize determinants in the usual Craig notation and the transformation behavior of the MO's of these determinants are as shown, i.e., the  $t_2 \eta$  MO transforms as product function  $yz$ , the  $t_2 \zeta$  as  $xy$ , etc.<sup>10</sup> These state components are substituted into the  $A/D$  expression, determinants are brought into maximum coincidence, and expressions such as

$$\frac{A}{D}(t_2^6 \rightarrow t_2^5 a_1^*) = -i \langle t_2 \eta | \hat{L}_z | t_2 \xi \rangle$$

are obtained. Other excitations are handled entirely alike.

### Results and Discussion

The electronic and MCD solution spectra are shown in Figures 2 ( $[\text{HgCl}_4]^{2-}$  and  $[\text{HgBr}_4]^{2-}$ ) and 3 ( $[\text{HgI}_4]^{2-}$ ). The latter figure also shows the mull spectra of  $(\text{NMe}_4)_2[\text{HgI}_4]$ .

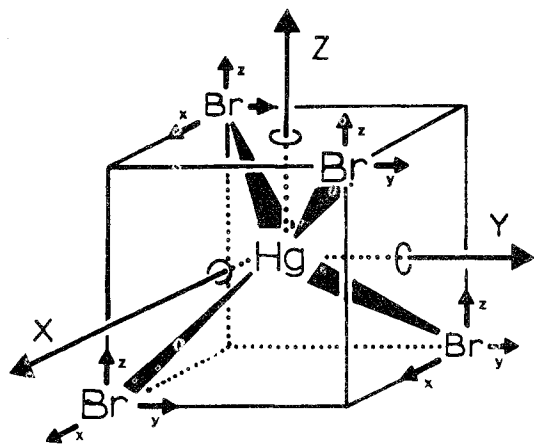


Figure 1. The molecular ( $X, Y, Z$ ) and local ( $x, y, z$ ) cartesian coordinate systems of  $[\text{HgBr}_4]^{2-}$ .

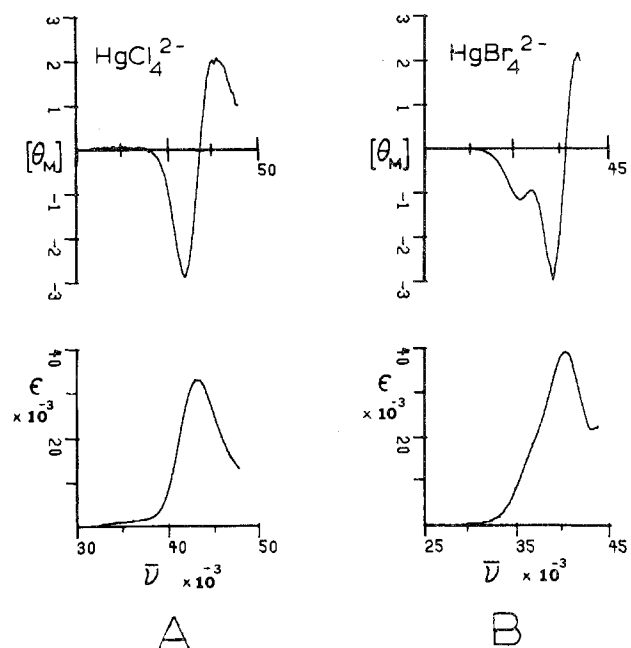


Figure 2. MCD and electronic absorption spectra of  $[\text{HgCl}_4]^{2-}$  (A) and  $[\text{HgBr}_4]^{2-}$  (B) in solution (see Experimental Section).  $[\theta]_M$  is the molar ellipticity per gauss.

Table I. Intense Electronic Excitations of  $[\text{HgX}_4]^{2-}$

$X^-$	$\lambda_{\text{max}}$ , nm	$\bar{\nu}_{\text{max}}$ , kK	$\epsilon_{\text{max}}$	$D,^a D^2$	$A/D, \text{BM}$
$\text{Cl}^-$	232	43.10	32,930	37.8	+0.53
$\text{Br}^-$	250	40.00	38,980	52.2	+0.26
$\text{I}^-$	323	30.96	23,140	27.5	+0.72
	269	37.17	32,400 <sup>a</sup>	44	+0.14 <sup>b</sup>

<sup>a</sup> Estimated from data of ref 4. <sup>b</sup> The  $A$  parameter was obtained from our mull spectrum (an estimate).

The electric dipole strength,  $D$ , in Debyes squared ( $D^2$ ) and the MCD Faraday ratio,  $A/D$ , in Bohr magnetons (BM) of the intense bands are given in Table I. The KI solution spectra of  $[\text{HgI}_4]^{2-}$  (Figure 3) show that the MCD dispersion crosses the wavelength axis where the intense ( $\epsilon$  23,140) electronic band maximum is located at 323 nm (31.0 kK). The spectra cannot be taken any farther toward the ultraviolet region because the solvent medium (large excess  $\text{I}^-$ ) will interfere. However, the relative MCD and electronic band positions indicate the presence of a distinct positive Faraday  $A$  term for this band. By measuring the MCD and electronic absorption spectra of a Kel-F mull (Figure 3) of solid  $(\text{NMe}_4)_2[\text{HgI}_4]$ , it is possible to demonstrate that the higher energy intense band

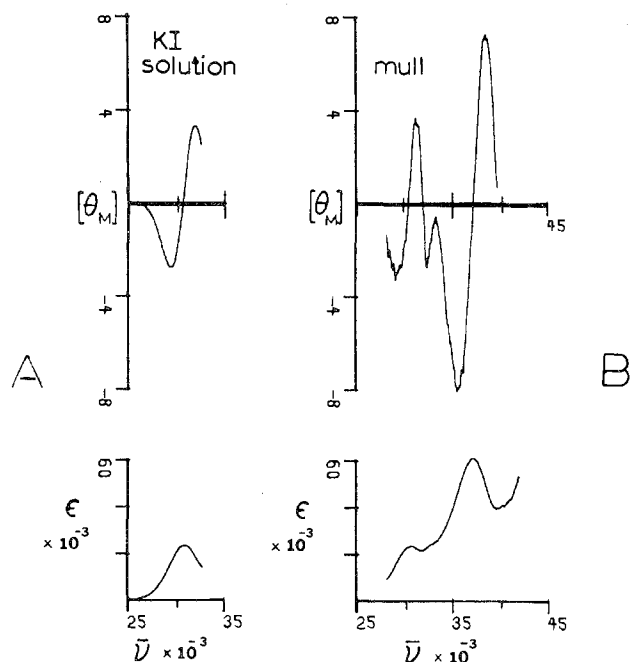


Figure 3. MCD and electronic absorption spectra of  $[\text{HgI}_4]^{2-}$  in aqueous 5 M KI solution (A) and of solid  $(\text{NMe}_4)_2[\text{HgI}_4]$  in a Kel-F mull (B). The ellipticity scale of the latter was used on the basis of knowing the  $\theta_{\text{max}}$  value of the 323-nm (31.0-kK) band of the  $[\text{HgI}_4]^{2-}$  solution spectrum.

at 269 nm (37.2 kK) also has a positive Faraday  $A$  term associated with it. The mull spectrum also shows the characteristic positive  $A$  term of the lowest energy intense band at 323 nm. We conclude that it is quite feasible to determine the shapes of MCD bands in mull media especially when these bands have very intense electric dipole strengths.

The relative positions of the lowest energy intense electronic and MCD bands of  $[\text{HgBr}_4]^{2-}$  (Figure 2) closely resemble the first band of  $[\text{HgI}_4]^{2-}$ . The intense electronic band maximum at 250 nm (40.0 kK) is 9.0 kK farther toward the ultraviolet region than its  $\text{I}^-$  analog. The distinct character of a positive Faraday  $A$  term is present again; i.e., the intensity of the MCD dispersion vanishes near the electronic band maximum. The shoulder near 280 nm on the electronic spectrum, which gives rise to the negative MCD activity, is probably spin forbidden in origin.

In  $[\text{HgCl}_4]^{2-}$ , we found that the  $\epsilon_{\text{max}}$  value at 232 nm (43.1 kK) was close to that reported previously.<sup>4</sup> This band maximum is 3.1 kK farther into the ultraviolet region than the bromo analog. Again, it is found that the MCD dispersion has vanishing intensity near the electronic absorption maximum, and the signs of the lobes define a positive  $A$  term (Table I).

As regards the nature of these excitations, the features of these first, or lowest energy, electronic absorption bands are consistent with charge-transfer bands, as the band intensities are very large and the band positions show a successive blue shift  $\text{I}^- < \text{Br}^- < \text{Cl}^-$  (Table I). This shift is characteristic of halogen-to-metal charge-transfer transitions. Furthermore, we take the orbital origin of the halogen electron to the  $\pi$ , or predominantly from  $\pi$  molecular orbitals localized on the halogen atoms (most molecular orbitals in  $T_d$  cannot be classified as  $\sigma$  or  $\pi$  bonding but one or the other can dominate). This assumption is based on (i) photoelectron spectra, e.g., as those by Green, Green, Joachim, Orchard, and Turner,<sup>11</sup> (ii) the blue shift of band maxima as the solvent is chosen to be more hydrogen bonding,<sup>4,12</sup> and (iii) the generally accepted view that lowest energy charge-transfer bands derive from the motion of electrons which come from molecular orbitals which

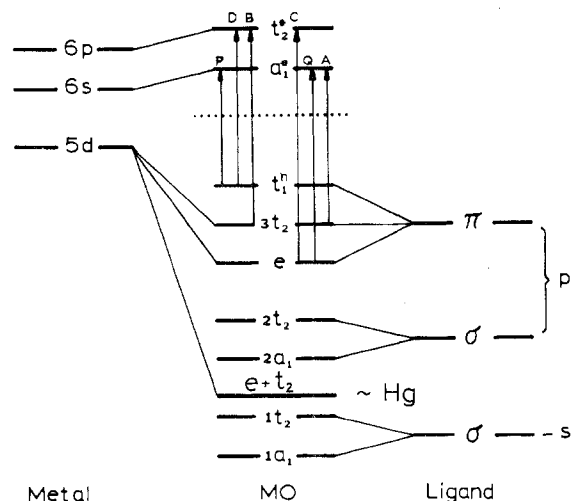


Figure 4. Schematic MO energy level diagram showing the six one-electron excitations from the ligand-localized  $\pi$  MO's. The order of filled  $\pi$  MO's,  $t_1 > 3t_2 > e$ , is as proposed in photoelectron spectra;<sup>12</sup> it is found from the calculations of the present study that the order of  $\pi$  MO's is  $3t_2 > e > t_1$ . However, the MCD interpretation does not depend on the order of one-electron MO's.

are energetically most easily ionized; i.e., electrons in  $\sigma$  bonds are more difficult to remove than those from ca. nonbonding  $p\pi$  orbitals.

The schematic  $[\text{HgX}_4]^{2-}$  MO diagram of Figure 4 shows that these deliberations still leave six excited configurations (A through D, and P and Q) to be examined. Above the

A	$3t_2^5 a_1^*$	D	$t_1^5 t_2^*$
B	$3t_2^5 t_2^*$	P	$t_1^5 a_1^*$
C	$e^3 t_2^*$	Q	$e^3 a_1^*$

dotted line of Figure 4 are the vacant MO's,  $a_1^*$  and  $t_2^*$ , where the former is composed largely of the 6s AO of Hg and the latter is largely of 6p Hg orbitals. The eight  $p\pi$  Br orbitals give rise to the  $3t_2$ ,  $t_1$ , and  $e$  MO's, of which  $t_1$  is nonbonding,  $e$  is 100%  $\pi$  bonding, and the  $3t_2$  MO is ca. 60%  $\pi$  bonding. Two of the six possible excited configurations, P and Q, can be eliminated from consideration immediately because their spin-allowed excited states,  $^1T_1$  and  $^1E$ , are forbidden by electric dipole selection rules; i.e.,  $[\text{HgX}_4]^{2-}$  complexes are closed-shell species so that only  $^1T_2$  excited states are allowed:  $\langle ^1A_1 | \hat{m} | ^1T_2 \rangle \in A_1$ ,  $m = er$  is the distance operator which transforms as  $T_2$ . However, each of the other four excited configurations, A–D, gives rise to several spin-singlet and spin-triplet states, including the electric dipole allowed one,  $^1T_2$  (Figure 5).

Since the electronic absorption data cannot be used to determine which excited configuration, A, B, C, or D, give rise to the lowest energy band of each  $[\text{HgX}_4]^{2-}$  complex, one must turn to the MCD spectra.

The experimental MCD finding of positive Faraday  $A$  terms for the lowest energy bands (Table I and Figures 2 and 3), makes this technique immediately quite complementary. Figure 5 also summarizes that only two of the possible four  $^1T_2$  state functions give rise to positive  $A/D$  ratios

$$A/D(^1T_2^B[3t_2^5 t_2^*]) = 0.73 \text{ BM}$$

$$A/D(^1T_2^C[e^3 t_2^*]) = 0.31 \text{ BM}$$

This leads to the conclusion that the lowest energy excitation of  $[\text{HgX}_4]^{2-}$  is to the  $t_2^*$  ( $\sim p$  Hg) MO, and the electron originates from one of the two  $\pi$  MO's,  $3t_2$  or  $e$ . Furthermore, the excitation into the  $a_1^*$  ( $\sim s$  Hg) MO can be excluded on the basis of the MCD data. On the same basis the MCD excludes from consideration transitions in which the electron

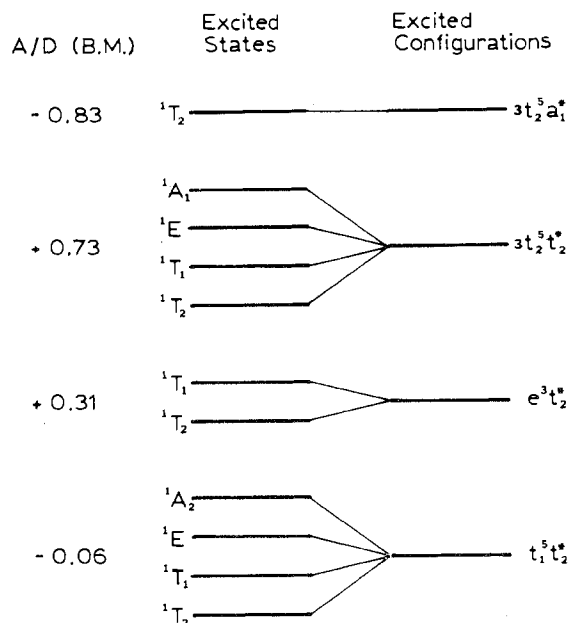
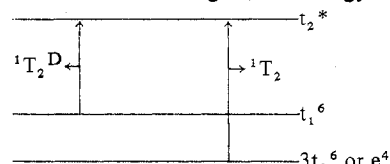


Figure 5. The spin-singlet excited states of four electric dipole allowed excited configurations. The Faraday  $A/D$  ratio of each  $^1T_2$  state is given in units of Bohr magnetons (BM).

originates from the third  $\pi$  MO, or  $t_1$ . It is quite interesting to note that PE spectroscopists<sup>11</sup> interpret that the highest energy, filled ligand-localized  $\pi$  molecular orbital is the  $t_1$   $\pi$  molecular orbital, not  $t_2\pi$  or  $e\pi$ . This might lead us to expect that the lowest energy band derives from the  $^1A_1 \rightarrow ^1T_2$  excitation  $t_1\pi \rightarrow t_2^*$  ( $t_1\pi \rightarrow a_1^*$  is forbidden). However, the MCD rules out this possibility and asserts that the lowest energy band is from  $t_2\pi \rightarrow t_2^*$  or  $e\pi \rightarrow t_2^*$ . We take this to infer that the lowest energy allowed orbital separation does not create the lowest energy state separation in this case. In other words, this is an exception to the simple anticipation that the relative magnitudes of energies between states parallel the order of one-electron MO energies; see energy level diagram



(also see Figure 4). In reality, we find  $^1T_2$ , not  $^1T_2D$ , is the lowest energy band; viz., for these transitions the order of orbital energy separations,  $\Delta\epsilon(t_2^* - t_2, e)$  does not determine the order of related states, so that the Coulomb-exchange contribution ( $\Delta E = \Delta\epsilon_{a,j} - J_{a,j} + K_{a,j}$ ) must be paid close attention. Alternatively, we feel that the photoelectron orbital order,  $t_1 > t_2$ , is not absolutely established as yet, since orbitals  $t_1$  and  $3t_2$  have the same electron population. It is clear from MCD, however, that the lowest energy electronic excitation of  $[\text{HgX}_4]^{2-}$  is not of orbital origin  $t_1 \rightarrow t_2^*$ , but it is ascertained that it is of origin  $t_2 \rightarrow t_1^*$  or  $e \rightarrow t_1^*$ .

It is of some interest that the higher energy intense band of  $[\text{HgI}_4]^{2-}$  also has a positive MCD  $A$  term (Figure 3). We conclude that this band (269 nm; 37.2 kK) is the second one of the two excitations,  $^1A_1 \rightarrow ^1T_2^B[3t_2^5 t_2^*]$  or  $^1A_1 \rightarrow ^1T_2^C[e^3 t_2^*]$ , which have positive  $A/D$  ratios (Figure 5). Not enough information is available at the moment to assign the small shoulder at 308 nm (32.4 kK) in the electronic spectrum of the mull (Figure 3), but its MCD intensity,  $\theta_{\max} \approx -3.0$ , is quite intense relative to its electric dipole strength, so that it may be a spin-forbidden band.

In summary, the electronic absorption data alone of  $[\text{HgX}_4]^{2-}$  permit assignment of the lowest energy intense band

of each complex ion to one of four possible excitations,  $\pi(X) \rightarrow \sim 6s(\text{Hg})$  or  $\rightarrow \sim 6p(\text{Hg})$ . The interpretation of the MCD data narrows this to either the  ${}^1T_2^B[3t_2^5t_2^*]$  or  ${}^1T_2^C[e^3t_2^*]$  excited states, or  $\pi(X) \rightarrow \sim 6p(\text{Hg})$ . The higher energy intense band of  $[\text{HgI}_4]^{2-}$  was also observed, and because of its positive  $A$  term it is assigned to  ${}^1T_2^C$  or  ${}^1T_2^B$ .

**Registry No.**  $[\text{HgCl}_4]^{2-}$ , 14024-34-1;  $[\text{HgBr}_4]^{2-}$ , 15906-07-7;  $[\text{HgI}_4]^{2-}$ , 14876-64-3;  $(\text{NMe}_4)_2[\text{HgI}_4]$ , 33615-18-8.

### References and Notes

- (1) Acknowledgment is made to the donors of the Petroleum Research Fund, administered by the American Chemical Society, for support of this research.
- (2) Y. Marcus, *Acta Chem. Scand.*, **11**, 599 (1957).
- (3) T. G. Spiro and D. N. Hume, *J. Am. Chem. Soc.*, **83**, 4305 (1961).
- (4) H. Fromherz and K. H. Lih, *Z. Phys. Chem., Abt. A*, **167**, 103 (1933).
- (5) R. Tsuchida, *Bull. Chem. Soc. Jpn.*, **13**, 388 (1938).
- (6) A. D. Buckingham and P. J. Stephens, *Annu. Rev. Phys. Chem.*, **17**, 399 (1966).
- (7) G. B. Deacon, *Rev. Pure Appl. Chem.*, **13**, 189 (1963).
- (8) As a representative computation of these tetrahedral  $[\text{HgX}_4]^{2-}$  molecules we chose the example of  $[\text{HgBr}_4]^{2-}$ . The internuclear Hg-Br distance was taken to be the sum of covalent radii, or 2.61 Å (see L. Pauling, "The Nature of the Chemical Bond", Cornell University Press, Ithaca, N.Y., 1960, p 246; C. L. V. P. Van Eck, H. B. M. Walters, and W. J. M. Jaspers, *Recl. Trav. Chim. Pays-Bas*, **75**, 802 (1956)). The multi- $\zeta$  metal basis functions (6s, 6p, 5d) of H. Basch and H. B. Gray, *Theor. Chim. Acta*, **14**, 367 (1966), and single- $\zeta$  bromine functions (4s, 4p) of E. Clementi and D. L. Raimondi, *J. Chem. Phys.*, **38**, 2686 (1963), were employed. Mercury (-13.0 eV, d; -9.7 eV, s; -5.5 eV, p) and bromine (-24.05 eV, s; -12.52 eV, p; H. Basch, A. Viste, and H. B. Gray, *Theor. Chim. Acta*, **3**, 458 (1965)) orbital energies were employed for diagonal elements of the molecular Hamiltonian matrix,  $\mathcal{H}$ , and off-diagonal elements were obtained with the Wolfsberg-Helmholz formula ( $K = 1.9$ ). Iterations were carried out until self-consistent Lowdin charges (see ref 9) were obtained.
- (9) R. S. Evans, A. F. Schreiner, and P. J. Hauser, *Inorg. Chem.*, **13**, 2185 (1974); A. H. Bowman, R. S. Evans, and A. F. Schreiner, *Chem. Phys. Lett.*, **29**, 140 (1974).
- (10) J. S. Griffith, "The Theory of Transition-Metal Ions", Cambridge University Press, Cambridge, England, 1961.
- (11) J. C. Green, M. L. H. Green, P. J. Joachim, A. F. Orchard, and D. W. Turner, *Philos. Trans. R. Soc. London, Ser. A*, **268**, 111 (1970).
- (12) C. K. Jorgensen, "Oxidation Numbers and Oxidation States", Springer-Verlag, New York, N.Y., 1969.

Contribution from the Quantum Chemistry Group, Uppsala University, 751 20 Uppsala 1, Sweden, and from the Department of Chemistry, Northeastern University, Boston, Massachusetts 02115

## Theoretical Study of the Chair-Boat Conformational Barrier in *cyclo*-Hexasulfur

ZELEK S. HERMAN<sup>1a</sup> and KARL WEISS<sup>\*1b</sup>

Received October 2, 1974

AIC40684Y

CNDO/2 molecular orbital calculations predict that the boat form of *cyclo*-hexasulfur exists and that its potential energy is ca. 4 kcal/mol less than that of the chair form which is found in the rhombohedral crystal. The interconversion has a barrier of 23 kcal/mol and is not forbidden by symmetry rules. A Mulliken population analysis provides a picture of the bonding in *cyclo*-hexasulfur which is consistent with thermodynamic data.

### Introduction

The stereochemistry of polysulfides is a topic of continuing interest.<sup>2</sup> In the case of elemental sulfur, the cyclic forms  $S_n$ ,  $n = 6, 8$ , and 12, are well-known and have been structurally characterized by X-ray methods.<sup>3</sup> Since it is the most stable form both in the crystal and in the vapor below 100°, most attention has been focused on  $S_8$  from both the experimental and the theoretical points of view.

One problem which has received only fleeting attention is that of ring inversion and structural isomerism in sulfur rings. *cyclo*-Hexasulfur is of greatest interest since, for this compound, a chair-boat interconversion can be envisioned. It has a chair conformation in the crystal. In comparing the conformational stabilities of cyclohexanes with those of polythianes it is found that the ease of ring inversion and flexibility decrease.<sup>4</sup> For pentathiane, a compound which resembles *cyclo*-hexasulfur, a conformational change has been observed at elevated temperature by NMR measurements.<sup>5</sup>

In this paper we examine the chair-boat interconversion of *cyclo*-hexasulfur by means of theoretical calculations. Previous calculations on sulfur ring compounds including *cyclo*-hexasulfur<sup>6-8</sup> have been primarily concerned with the participation of sulfur 3d orbitals in bonding and with spectral properties. The conformations of cyclic sulfur rings have also been studied from purely geometrical<sup>9</sup> and thermodynamic<sup>10</sup> points of view. We have chosen the all-valence electron CNDO/2 method<sup>11</sup> to establish the possible stability of the boat conformer of *cyclo*-hexasulfur, to estimate the inversion barrier, and to assay bonding relationships with the aid of a Mulliken overlap population analysis.<sup>12</sup>

### Calculations

The CNDO/2 version employed is based on the parametrization of Santry<sup>13</sup> modified<sup>14</sup> to ensure invariance to

molecular rotation. The basis set includes sulfur 3d orbitals. To accomplish the overlap population analysis,<sup>12</sup> the CNDO basis orbitals, which are orthogonal in the zero differential overlap approximation, are transformed into a nonorthogonal set.<sup>15</sup> This procedure provides overlap populations in test cases involving molecules of first-row atoms which are in good agreement with the results of ab initio calculations.

The bond lengths and bond angles of *cyclo*-hexasulfur used in this work are those determined experimentally<sup>16</sup> (sulfur-sulfur distance 2.057 Å, S-S-S bond angle 102.2°). To investigate the various conformations encountered in the chair-boat interconversion, only the angle  $\phi$  (cf. Figure 1) was varied. The bond lengths were kept constant since the CNDO/2 method appears to be most successful when experimental geometries are utilized.<sup>17</sup>

### Results

(a) **Energy Surface and Inversion Barrier.** In Figure 2 the nuclear energy and electronic energy are plotted as a function of the bending angle  $\phi$ . The curves were, in each case, obtained from the 13 calculated points using a standard interpolation procedure.<sup>18</sup> Nuclear energy refers to the nuclear-nuclear repulsion energy of all the sulfur nuclei within the Born-Oppenheimer approximation, while electronic energy refers to the sum of the electronic kinetic energy, the electronic-electronic repulsion energy, and the electronic-nuclear attraction energy. The total energy is the sum of the nuclear and electronic energies since relativistic effects are neglected in the CNDO/2 approximation.

While the nuclear energy and electronic energy vary considerably as a function of the angle  $\phi$ , their sum is very nearly constant (Figure 2). The strong angular dependence of these energy components can be understood in terms of the variation of the internuclear distances and overlaps for the